JOURNAL OF CATALYSIS 102, 140–150 (1986)

# Mechanism of Methane Formation in Potassium Catalyzed Carbon Gasification

C. A. MIMS[1] AND J. J. KRAJEWSKI

*Exxon Research and Engineering Company, Corporate Research Science Laboratories, Clinton Township, Route 22 East Annandale, New Jersey 08801*

Received March 23, 1986; revised June 17, 1986

We have performed a kinetics and isotope tracer study of the mechanism of $CH_4$ formation from a potassium catalyzed carbon during gasification in atmospheres containing $H_2O$, $H_2$, $CO_2$, and CO Temperatures from 925 to 1025 K and pressures up to 8 atm were studied. We found that although potassium salts catalyze the formation of $CH_4$, there is not a one-to-one correspondence between $CH_4$ and CO formation rates implying different sites for generation of the two products. At low gas phase carbon activity the $CH_4$ product is formed by direct hydrogenation of substrate carbon and not by secondary reaction of gas phase CO or $CO_2$. At higher gas phase carbon activities some $CH_4$ is produced from gas phase carbon oxides as a result of carbon deposition. In some cases the deposited carbon shows higher reactivity than the original carbon substrate so that this can be legitimately viewed as a secondary pathway.

## I. INTRODUCTION

The catalysis of carbon gasification by alkali salts has been studied extensively (*1*). However, most of the fundamental studies to date have addressed the mechanism of CO formation while the pathway of the $CH_4$ formed during the catalyzed $H_2O$–carbon reaction has received little attention.

The possible pathways for $CH_4$ production include (1) direct reactions of carbon or carbon surface intermediates with $H_2O$ or $H_2$ and (2) secondary reactions in which gas phase CO or $CO_2$ are catalytically reduced to $CH_4$. A detailed study of $CH_4$ production kinetics from Pt-catalyzed carbon led Holstein and co-workers to conclude that the $CH_4$ came from a direct reaction of $H_2O$ with the carbon substrate (*2*). For alkali catalysis very little is known about $CH_4$ formation. Gilliland *et al.* (*3*) found that $CH_4$ was near gas phase equilibrium values during the potassium catalyzed $H_2O$–carbon reaction, revealing little mechanistic information. Several studies have shown that alkali salts promote the reaction of hydrogen with coals and chars (*4, 5*) indicating that direct hydrogenation of carbon is a viable pathway for methane production. Methane is also produced by contacting CO–$H_2$ mixtures with alkali salt promoted carbons (*6, 7*). The production of methane by direct reaction of $H_2O$ with graphite was reported to be efficiently promoted by KOH at 525 K (*8*), a finding that was not reproduced in subsequent studies (*9*).

Understanding the mechanism of $CH_4$ formation is important whether the molecule is considered to be a desirable or undesirable product in carbon gasification. We have performed a steady-state kinetics and tracer study of $CH_4$ formation during the potassium catalyzed $H_2O$–carbon reaction near 1000 K. The influence of catalyst concentration and carbon conversion on the $CH_4$ production rate were compared with their effect on the CO production rate to determine if there is any relationship between the sites for the two reactions. We examined the dependence of $CH_4$ production on gas composition in atmospheres containing $H_2O$, $H_2$, CO, and $CO_2$. We also used $^{13}C$-labeled CO and $CO_2$ to distinguish $CH_4$ produced directly from the carbon lat-

[1] To whom correspondence should be addressed.



0021-9517/86 $3.00

tice from that produced by a secondary reaction pathway.

## II. EXPERIMENTAL METHODS

The experiments were performed in a stainless-steel tubular flow reactor which was quartz-lined to avoid methane formation on the metal walls. Water vapor was prepared by passing oxygen with excess hydrogen over a supported platinum catalyst. Metered flows of the other components were added to the resulting $H_2O$–$H_2$ mixture to produce the desired reactant gas composition. A heated zone enclosing both the reactant and product gas lines assured that water remained in the vapor phase.

The water gas shift reaction

$$H_2O + CO \rightarrow CO_2 + H_2 \qquad (1)$$

is rapidly equilibrated over potassium catalyzed carbons under the conditions of this study (*3, 10*). If the water gas shift reaction is in equilibrium, this reduces by one of the number of variables necessary to specify the gas composition. Any gas atmosphere containing CO, $CO_2$, $H_2O$, and $H_2$ with the same H/C/O composition is identical after equilibration of the shift reaction. As a practical matter, we generally produced the desired gas composition from $H_2$, $H_2O$, and $CO_2$ and allowed shift equilibration to occur at the top of the bed. Methanation rates in these atmospheres prepared from three components were found to be identical to those synthesized from four components to be in shift equilibrium. This finding validated the simplified treatment used here. The rates were measured under differential conditions with respect to CO, $CO_2$, $H_2$, and $H_2O$ concentrations. The methane concentrations generated were too small to influence the concentrations of the other four components and were always much less than an equilibrated mixture of the same H/C/O composition.

The rates were measured by GC analysis of the product gas; the isotopic composition of the $CH_4$ in the tracer experiments were measured by GCMS. We examined a high purity model carbon in this study (Spherocarb, Analabs, Inc.). The potassium was added as enough $K_2CO_3$ solution to fill the pores of the dry solid.

The effects of gas composition on the rate were treated as separable from those of the other variables, i.e.,

$$R_{CH_4} = Q(P_{CO}, P_{CO_2}, P_{H_2}, P_{H_2O}) \cdot R_0 \quad (\text{K/C, carbon conversion etc.}). \qquad (2)$$

In measuring the rate law $Q$, the $CH_4$ production rates were time normalized by returning to a standard gas composition to account for changes in $R_0$, the rate at the standard gas composition. Standard gas compositions were used to examine the effects of the other variables. Although separability is not justified *a priori* (the gas composition could affect the shape of the carbon conversion curve, for example) we did not notice any strong coupling under our conditions. To simplify the analysis we present data on the gas phase composition dependence which were collected over a limited range of carbon conversion (20–50%).

## III. RESULTS

### *$CH_4$ Formation Kinetics: Dependence of Catalyst Concentration*

The presence of potassium gasification catalyst increases the rate of methane formation over Spherocarb. Figure 1a shows the rate of methane formation from a standard gas mixture (H/C/O = 8/4/1, $P$ = 3.5 atm) over Spherocarb to which different amounts of catalyst had been added. Prior to $CH_4$ measurements these samples were reacted in a 2 : 1 $H_2O$–$H_2$ mixture at 975 K to achieve ~10% carbon conversion. The total gasification rates (mostly CO + $CO_2$) measured just prior to the $CH_4$ measurements are shown in Fig. 1b.

The dependence of the $CH_4$ formation rate on catalyst concentration is similar to that for the total gasification rate. Initial amounts of potassium salts catalyze $CH_4$ formation. Above a certain level additional

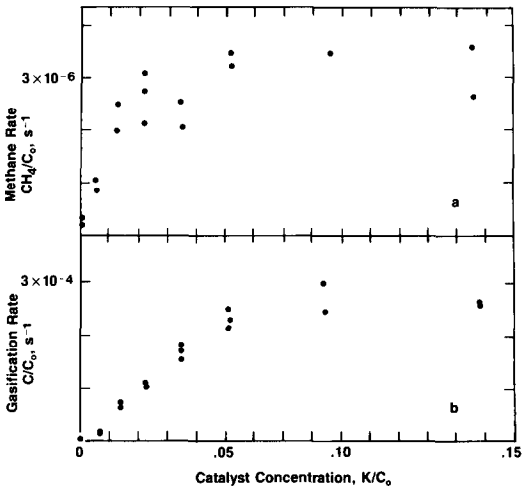


FIG. 1. Response of initial gasification and methanation rates to catalyst concentration on Spherocarb. Upper panel: methane production rate measured at 975 K, total pressure 4.5 atm, gas composition H/C/O = 0.593/0.111/0.296 ($pH_2$ = 1.9 atm). $C_0$ = initial carbon content in sample. Lower panel: total gasification rate measured at 975 K, total pressure 4.5 atm, $H_2O/H_2$ = 2.0 measured just prior to $CH_4$ rates in upper panel.

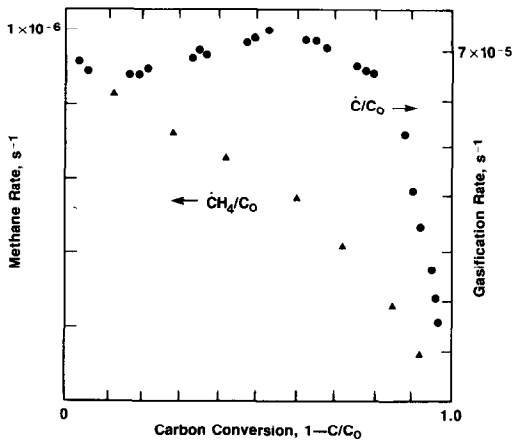


FIG. 2. Comparison of methane formation with total gasification rate as catalyzed Spherocarb is gasified. K/C = 0.028, 975 K, total pressure = 1.80 atm. Left axis is methane production rate per original carbon in sample measured with gas composition H/C/O = 0.552/0.103/0.345 ($p_{H_2}$ = 0.51 atm). Right axis is gasification rate measured with $H_2O/H_2$ ratio = 1.0.

catalyst does not produce an additional increase in rate. A similar effect which has been reported previously, is shown in the total gasification rate (*11, 12*).

The absolute $CH_4$ production rates are low compared to the CO production rates at the conditions used here. Because different rate laws apply to the two processes, the rate of $CH_4$ production can be comparable to CO production at higher pressures.

### *Comparison of CO and $CH_4$ Production Rates*

Although qualitatively similar, the catalyst concentration dependences shown in Fig. 1 for the two reactions do not follow one another quantitatively. The methane formation rate appears to saturate at a lower catalyst concentration than the total gasification rate. This implies that there is not a one-to-one correspondence between the sites for the two reactions. We examine this point more closely in Figs. 2 and 3. Figure 2 compares the methanation rate with $CO_x$ production rates as one catalyzed sample is burned out. The rates were measured as described in the previous section by cycling between the two gas atmospheres. For this catalyst concentration

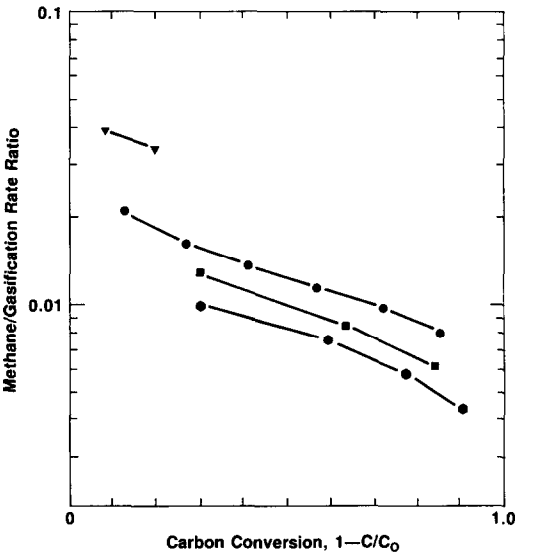


FIG. 3. Ratio of methane formation rate to total gasification rate versus carbon conversion for several catalyzed carbons. Rates were measured as in Fig. 3. ▼ = Spherocarb (K/C = 0.013), ● = (K/C = 0.028), ■ = (K/C = 0.052), ⬢ = (K/C = 0.139).

and gas composition and pressure, the total gasification rate is approximately zero order in carbon until >80% conversion whereas the $CH_4$ rate drops steadily with carbon conversion.

The ratio of methanation/gasification rates is plotted in Fig. 3 versus carbon conversion for several samples of Spherocarb. Not only does the rate ratio decrease as each sample is converted but the ratio at a given carbon conversion depends on catalyst concentration. This could reflect variation in the relative number and/or activity of $CH_4$ production sites. Thus, it is clear that although the presence of alkali salts provides $CH_4$ production sites, a simple one-to-one correspondence of methanation and CO production does not exist.

### *$CH_4$ Kinetics: Dependence on Gas Composition*

The inlet gas compositions used in this study are plotted on an H/C/O composition diagram in Fig. 4. A position on this diagram is sufficient to specify the mole fractions of $H_2O$, $H_2$, CO, and $CO_2$ at a given temperature at water-gas shift equilibrium.

Consideration must be given to the gas composition with respect to carbon (graphite) deposition via the Boudouard reaction.

$$2CO \rightarrow CO_2 + C_s(\text{graphite}) \quad (3)$$

or the reverse $H_2O$–C reaction.

$$H_2 + CO \rightarrow H_2O + C_s(\text{graphite}). \quad (4)$$

With the gas phase in shift equilibrium the carbon activity of the gas ($\alpha_g$) with respect to Reactions (3) and (4) is identical and equal to

$$\alpha_g = \frac{K_3 P_{CO}^2}{P_{CO_2}} = \frac{K_4 P_{H_2} P_{CO}}{P_{H_2O}} = \frac{K_1 K_4 P_{CO}^2}{P_{CO_2}} \quad (5)$$

where $K_1$, $K_3$, and $K_4$ are equilibrium constants for Reactions (1), (3), and (4), respectively. The carbon deposition line ($\alpha_g = 1$) for 973 K and 5 atm total pressure is shown as a dashed line in Fig. 4. All references in this paper to the gas phase carbon activity relate to Eq. (5) and do not include $CH_4$. The methane rates are all measured far from C–$H_2$ equilibrium.

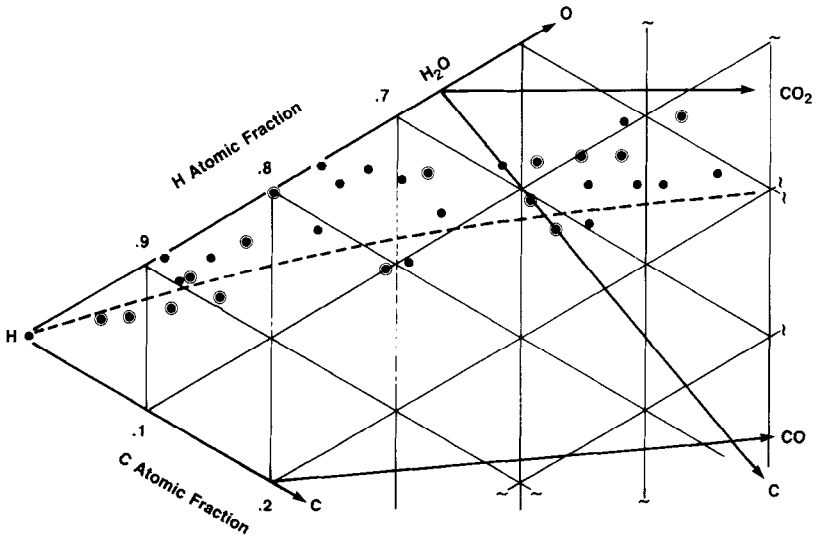


FIG. 4. Compositions used in the study plotted on a portion of an H/C/O composition diagram: methanation kinetics were measured at all compositions, tracer experiments were performed at circled compositions. The dashed line is the graphite deposition line for 975 K and 5 atm total pressure.

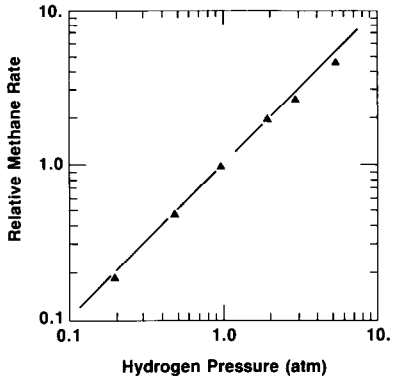


FIG. 5. Hydrogen pressure dependence of methane formation rate in pure hydrogen. ▲ = Spherocarb (K/C = 0.028). Solid line has first order slope.

### *$CH_4$ Formation Kinetics in Pure Hydrogen*

The kinetics of the catalyzed C–$H_2$ reaction (without oxygen-containing gas phase constituents) were examined separately as a subset of the gas compositions. Figure 5 shows that the reaction exhibits a first order dependence on hydrogen pressure. The $CH_4$ production rates were normalized to 1 atm. This normalization was required by the decay of the $CH_4$ formation rate with time at low to moderate pressures (shown in Fig. 6). Since the gasification rates are quite slow in low pressure (1 atm) $H_2$, this deactivation takes place while very little carbon is converted. Upon reintroduction of a $H_2O$–$H_2$ mixture, the $CH_4$ rate returns to roughly the same value as it had before the $H_2$ reaction period. Upon reintroduction of pure $H_2$ reactant, the previous rate is restored. This rate decays in a similar manner to the previous period (Fig. 6). This cycle can be repeated many times. No significant catalyst loss is observed during the $H_2$ reaction period, a fact which is reinforced by the return of the rate in $H_2O$–$H_2$ to its original value. The maintenance of steady $CH_4$ production obviously depends on some attribute of the oxidizing environment.

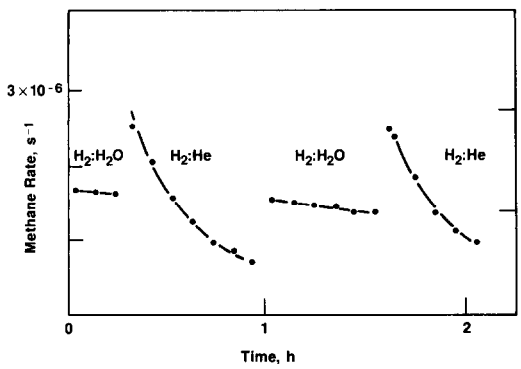


FIG. 6. Deactivation of hydrogen gasification rate with time and subsequent reactivation in $H_2O/H_2$ mixture. All reactant gas ratios = 1 : 1, $T$ = 975 K, 1.4 atm total pressure. Spherocarb (K/C = 0.028).

### *$CH_4$ Formation Kinetics in Multicomponent Mixtures*

Figure 4 shows the gas compositions used in the kinetics study. Most of the data were taken at 975 K at total pressures of 1.5, 4.5, and 7 atm total pressure although not all compositions were used at each pressure. A small subset of compositions was used to investigate the effect of temperature. A multivariate regression was not attempted on the data. It was found that the rate data correlated in an explainable way with the hydrogen partial pressure and gas phase carbon activity. Figure 7 shows that the relative methanation rate at 975 K has approximately first order dependence on hydrogen pressure for gas atmospheres for which the gas phase carbon activity is low ($\alpha_g < 0.5$). Rates in gas atmospheres with higher carbon activity (open points in Fig. 7) lie consistently higher than the rest of the data.

We define the first order methane reactivity, $\rho$, as

$$\rho = Q/p_{H_2} \qquad (6)$$

where $Q$ is the relative rate defined in Eq. (2). In Fig. 8, we plot $\rho$ versus the gas phase carbon activity. A horizontal line reflects simple first order kinetics. The data show a region of simple first order hydrogen dependence with a positive deviation at higher carbon activities. The curves drawn in Fig.

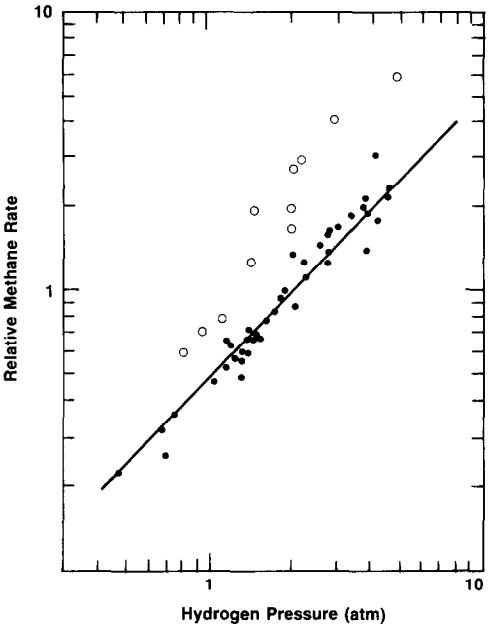


FIG. 7. Dependence of methane formation rate on hydrogen partial pressure in multicomponent mixtures. Rates are relative to those under standard conditions (H/C/O = 0.593/0.111/0.296, total pressure = 4.5 atm). Open circles represent atmospheres with carbon activity > 0.5. Solid line has first order slope.

8 are predictions of a simple model which we discuss later. The cluster of data at low carbon activities are for $H_2O$–$H_2$ atmospheres where the only CO or $CO_2$ present is that generated by gasification. These data are scattered, but seem to be somewhat above the average first order correlation. This could reflect a modest inhibition in the rate by CO or $CO_2$ which is unaccounted for in this analysis.

*Temperature Dependence*

The temperature dependence of the methane formation rate was measured in a cursory fashion for several gas compositions. These rates are normalized to a standard condition and plotted in Fig. 9. The first order rate coefficients in multicomponent gas mixtures are fit with an activation energy of approximately 34 kcal/mole. A similar temperature dependence characterizes the methane formation rate at lower temperatures than those in Fig. 10. At 525 K in $H_2O$ and $H_2O$–$H_2$ we always measured turnover frequencies ($CH_4/K^+ \cdot s$) less than $10^{-8}$ compared to $3 \times 10^{-3}$ reported in Ref. (*8*). We measured rates at 825 K which were in reasonable agreement with the data in Ref. (*9*).

*Isotope Tracer Experiments*

A series of tracer experiments were performed at 1.5, 4.5, and 7 atm at the compositions shown by the circled dots in Fig. 4.

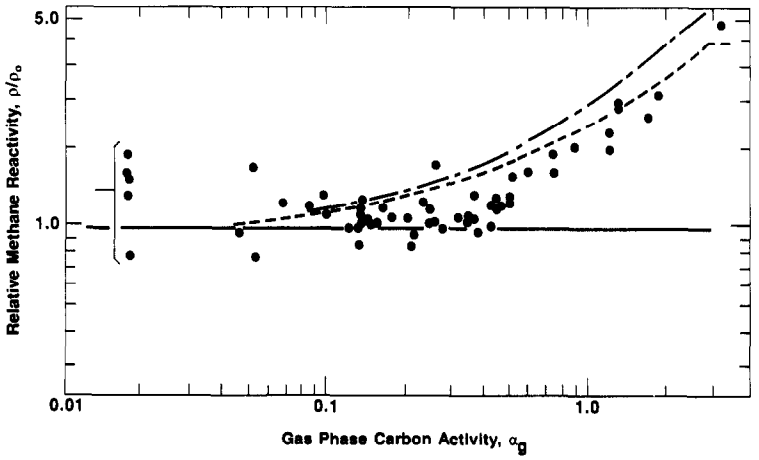


FIG. 8. First order methane rate coefficient (relative to that at standard conditions) plotted versus gas phase carbon activity. ● = Spherocarb (K/C = 0.028). Temperature = 975 K. Curves are generated from the model discussed in the text using the following parameters: — ($\alpha_c$ = 1, $\beta$ = 1), --- ($\alpha_c$ = 3, $\beta$ = 5), -·-· ($\alpha_c$ = 25, $\beta$ = 50).

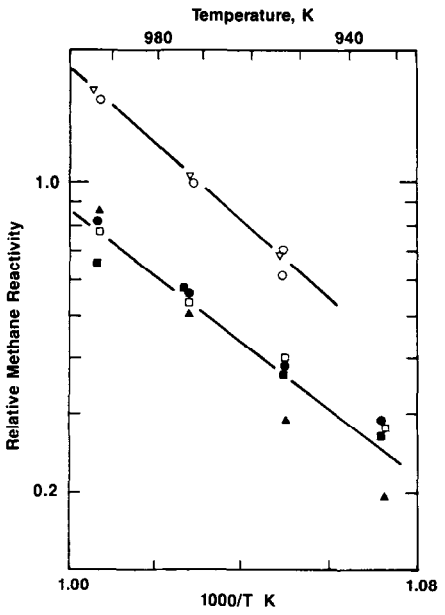


FIG. 9. Temperature dependence of the first order methane formation rate from several gas compositions over Spherocarb (K/C = 0.028). All except those in pure hydrogen are measured relative to standard composition at 975 K. The total pressure was 1.8 atm. Gas compositions (□ = H/C = 0.485/0.152, ● = 0.762/0.048, ■ = 0.598/0.111, ▲ = 0.522/0.103, ▽ = $H_2O/H_2$ = 1.0, ○ = pure $H_2$.

The use of $^{13}CO$–$^{13}CO_2$ in the reactant gas shows how much $CH_4$ resulted from conversion of gas phase carbon oxides. The fraction of $CH_4$ derived from the gas phase at 975 K is plotted versus carbon activity in Fig. 10. The fraction of labeled methane did not show a simple correlation with the partial pressure of any other gas phase constituent.

These results show that most of the $CH_4$ comes directly from the carbon substrate at low carbon activities. The rate law and reactivity in the multicomponent mixtures is the same as that in pure hydrogen. Therefore, the reaction proceeds by a direct hydrogenation of carbon atoms of the substrate. The transient behavior shown in Fig. 6 indicates that carbon atoms are activated for $CH_4$ formation at these conditions by the chemistry associated with gasification in $CO_2$–$H_2O$. These activated carbon sites deactivate in pure $H_2$ and may be associated with surface oxygen or other intermediates as yet unidentified.

At higher carbon activities more of the $CH_4$ carries the gas phase label until at carbon activities greater than unity almost all of the $CH_4$ is derived from gas phase carbon oxides. The appearance of $^{13}CH_4$ is expected at high carbon activities where the reverse of the $H_2O$–C and $CO_2$–C gasification reactions is significant and contaminates the substrate with $^{13}C$. A simple

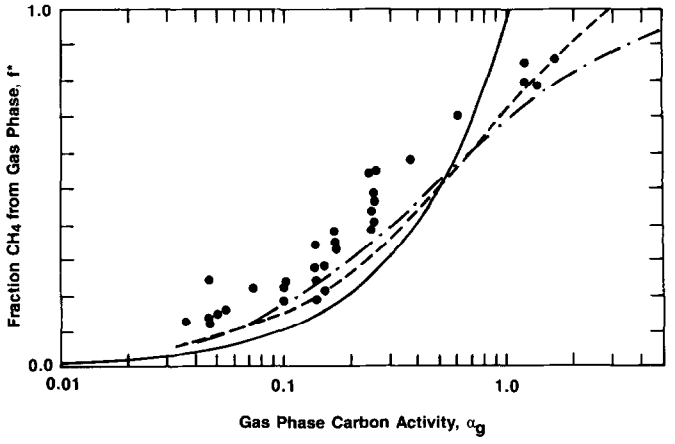


FIG. 10. Fraction of methane is formed from gas phase carbon oxides as a function of gas phase carbon activity. ● = Spherocarb (K/C 0.028). Curves are generated from the model discussed in the text with the following parameter values: — ($\alpha_c = 1, \beta = 1$), --- ($\alpha_c = 3, \beta = 5$), –·–· ($\alpha_c = 25, \beta = 50$).

model developed here explains the major trends with carbon activity and gives a semiquantitative value of the amount of labeled $CH_4$ expected from the reversible gasification of the carbon substrates.

## IV. KINETIC MODEL

In the kinetic model, $CH_4$ results from the reaction of $H_2$ with a constant number, $S$, of surface carbon sites. These sites are modeled as last-in-first-out stacks of carbon atoms which are in dynamic balance between the forward and reverse $H_2O$–carbon and $CO_2$–carbon reactions.

$$\begin{aligned} \cdot CC + H_2O(CO_2) &\xrightarrow{R_f} \cdot CC + CO + H_2(CO) \\ \cdot CCC^* + H_2O(CO_2) &\underset{R_b}{\overset{R_f}{\rightleftarrows}} \cdot CC + {}^*CO + H_2(CO) \\ \cdot CCC^*C^* + H_2O(CO_2) &\underset{R_b}{\overset{R_f}{\rightleftarrows}} \cdot CCC^* + {}^*CO + H_2(CO) \text{ etc.} \end{aligned} \tag{7}$$

Carbon atoms gasify to produce CO with *specific rate* $R_f$ and are deposited at rate $R_b$. In the deposition step the oxygen atom is rejected as $CO_2$ or $H_2O$. If the gas phase carbon is labeled, the deposition step results in the incorporation of a label onto the site. The set of steady-state equations generated by the above,

$$d(\cdot CCC^*)/dt = 0 = -R_f(\cdot CCC^*) + R_b(\cdot CC) + R_f(\cdot CCC^*C^*) \text{ etc.} \tag{8}$$

can be solved to yield $\theta^*$, the fraction of sites which are labeled. In the case that $R_b < R_f$, this fraction is simply $R_b/R_f$, the ratio of the reverse to the forward rates.

The labeled and unlabeled sites are assumed to react with hydrogen to give $^*CH_4$ and $CH_4$.

$$\begin{aligned} \cdot CCC^*, \cdot CCC^*C^*, \text{ etc. } + 2H_2 &\rightarrow {}^*CH_4 \\ \cdot CC + 2H_2 &\rightarrow CH_4 \end{aligned} \tag{9}$$

Methane production rates are slower than CO production under the conditions of this study and are therefore assumed to have no effect on the surface isotopic composition. Under this assumption the rates of $CH_4$ and $^*CH_4$ production are given by first order rate constants $k$ and $k^*$, respectively.

$$\begin{aligned} {}^*\dot{CH}_4 &= S \cdot k^* \cdot \theta^* \cdot p_{H_2} \\ \dot{CH}_4 &= S \cdot k \cdot (1 - \theta^*) \cdot p_{H_2}. \end{aligned} \tag{10}$$

Combination of Eqs. (10) and the expression for $\theta^*$ yields the following expression for $f^*$, the fraction of $CH_4$ carrying the gas phase label,

$$\begin{aligned} f^* &= \beta\gamma/(1 + (\beta - 1)\gamma), \quad \gamma \le 1 \\ &= 1, \qquad\qquad\qquad \gamma \ge 1 \end{aligned} \tag{11}$$

where $\beta = k^*/k$ and $\gamma = R_b/R_f$. If $\rho_0$ is the limiting rate coefficient (see Eq. (6)) at low carbon activities where $R_b \ll R_f$ the expression for the methanation reactivity, $\rho$, relative to $\rho_0$ is

$$\begin{aligned} \rho/\rho_0 &= (\beta - 1)\gamma + 1, \quad \gamma \le 1 \\ &= \beta, \qquad\qquad \gamma \ge 1 \end{aligned} \tag{12}$$

The model assumes that reversible gasification affects all sites involved in $CH_4$ formation site. Since the potassium catalyst is believed to be mobile (*1*, *13*) and $CH_4$ formation is associated with the presence of catalyst, this assumption is probably not a bad one for this system, although some non-steady-state effects could play a role.

Evaluation of $\gamma$ (the ratio of reverse to forward rates) requires knowledge of the forward and reverse rate laws. For atmospheres in $H_2O$–C and $CO_2$–C equilibrium $\gamma$ is, of course, 1. Away from equilibrium the ratio of reverse and forward rates is given in general $\gamma = (\Pi_i/K_{eq})^s$ where $\Pi_i$ is shorthand for the mass action activity quotient, $K_{eq}$ is the equilibrium constant for the reaction in question, and $s$ is an arbitrary exponent (*14*). For the reaction of $2CO \rightarrow$ graphite + $CO_2$

$$\gamma = (K_4 P_{CO}^2/P_{CO_2})^s = \alpha_g^s \tag{13}$$

where $\alpha_g$ is the gas phase carbon activity

given in Eq. (5). Similar reasoning holds for the $H_2O$–C reaction. It has been shown that char-like carbons can sustain gas phase carbon activities greater than unity under the conditions of this study. Solid carbon activities of 2–4 are typical (*15*). When the gas phase is assumed to be reacting with a carbon with activity $\alpha_c$ the expression for $\gamma$ becomes $\gamma = (\alpha_g/\alpha_c)^s$.

The exponent $s$ can be evaluated directly by measuring the pressure dependence of scrambling of lattice carbon with gas phase carbon at gas–carbon equilibrium. We have not done this but rely on measured rate laws for the forward and reverse reactions far from equilibrium. The forward rate laws for the $K^+$-catalyzed $H_2O$–carbon and $CO_2$–carbon reactions have been previously reported as being well given by $R_f \propto [CO_2]/[CO]$ and $R_f \propto [H_2O]/[H_2]$ at compositions corresponding to those with $\alpha_g \approx 1$ in this study (*11, 16*). The rate law for the reverse reaction has not been reported for any conditions. Figure 11 shows a first order CO pressure dependence for carbon deposition when pure CO reactant is flowed over catalyzed Spherocarb. There was no change in the rate with reactant flow rate to indicate a $CO_2$ pressure dependent term in the rate expression. A first order rate law for $R_b$ combined with the gasification rate laws gives

$$\frac{R_f}{R_b} \propto \frac{P_{CO_2}}{P_{CO}^2} \propto \frac{P_{H_2O}}{P_{CO}P_{H_2}}. \tag{14}$$

The exponent $s$ in Eq. (13) is therefore unity and $\gamma = \alpha_g/\alpha_c$. Equations (11) and (12) now become

$$\begin{aligned} f^* &= \alpha_g\beta/(\alpha_c + \alpha_g(\beta - 1)), && \alpha_g < \alpha_c \\ &= 1, && \alpha_g > \alpha_c \end{aligned} \tag{15}$$

and

$$\begin{aligned} \rho/\rho_0 &= \alpha_g(\beta - 1)/\alpha_c + 1, && \alpha_g < \alpha_c \\ &= \beta, && \alpha_g > \alpha_c \end{aligned} \tag{16}$$

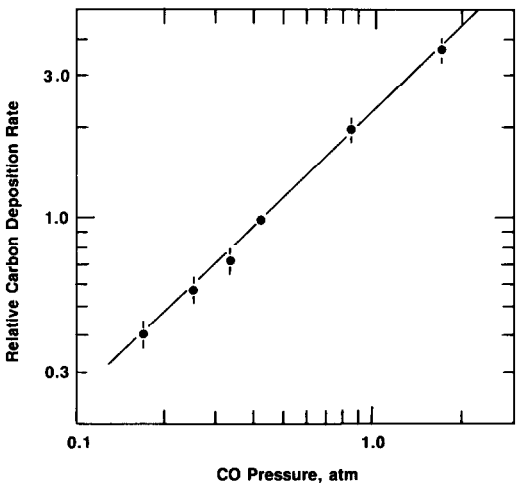


FIG. 11. Relative carbon deposition rates on catalyzed Spherocarb (975 K, K/C = 0.028) in pure CO reactant versus CO pressure. Solid line has first order slope.

*Comparison of Model with Data*

Curves generated from Eqs. (15) and (16) are compared with the data in Figs. 8 and 10. Within the context of this model these curves indicate how much of the labeled methane can be explained by reversible reaction of the carbon substrate. The simplest case is that where the substrate carbons and deposited carbons are equally reactive ($\beta = 1$). The solid curves in the figures are generated assuming that both $\beta$ and the solid carbon activity, $\alpha_c$, are unity. A higher solid carbon activity simply shifts the curves for a given $\beta$ to higher carbon activities along the logarithmic $x$ axis in Figs. 8 and 10. for Spherocarb, a value of $\beta$ near 2 gives the best fit with $\alpha_c = 1$.

A solid carbon activity of 2–4 is more appropriate to these carbon samples and better fits to the data are obtained by using values of $\alpha_c$ in this range. An increase in the carbon activity requires an increase in $\beta$ for a good fit. For $\alpha_c = 3$ the data are best fit with $\beta = 5$. The curves generated by this combination of parameters are shown as dashed lines in Figs. 8 and 10. Within the context of the model $\beta > 1$ means the deposited carbon atoms are more reactive for hydrogenation than the substrate.

The data can be reasonably well fit by

much higher values of $\beta$ with concomitant high values of $\alpha_c$. One such fit ($\alpha = 25$, $\beta = 50$) is shown in Figs. 8 and 10 as dot–dash curves. It is difficult to give physical meaning to such high values of $\alpha_c$ within the context of the model since the carbon intermediate which gives rise to $CH_4$ is in dynamic balance with the carbon substrate and the char carbon activities are 2–5.

## V. DISCUSSION AND SUMMARY

The dominant mode of methane formation at low gas phase carbon activities is by direct hydrogenation of carbon from the substrate. The reaction is catalyzed by the presence of alkali salt gasification catalysts. Although we did not observe higher molecular weight hydrocarbons at our conditions, it is possible that those observed in Ref. (*9*) at 825 K from the potassium catalyzed $H_2O$–graphite reaction are also the result of hydrogenation of the graphite substrate by the major product hydrogen. The uncatalyzed reaction of hydrogen with graphite to produce $C_2^+$ hydrocarbons as well as $CH_4$ at temperatures near 800 K has been reported (*17*).

At higher gas phase carbon activities, CO and $CO_2$ are converted to $CH_4$. The results of the model calculations show that most of this "indirect" methane can be plausibly accounted for by considering carbon deposition from the gas phase. To fit the data well, the deposited carbon has to be assumed to be more reactive than the substrate. Therefore, the formation of $CH_4$ from CO and $CO_2$ is a kinetically distinguishable pathway and could legitimately be viewed as a chemically distinct indirect path.

We have shown that the reactivity depends on the degree of carbon conversion and presumably, initial carbon substrate. This contrasts with the relative insensitivity of the CO producing gasification reactions. This variability in reactivity makes it difficult to draw a chemical distinction between direct and indirect $CH_4$ production since the deposited carbon can be viewed as another in the class of charlike carbons. The reactivity of the deposited carbon differs from that of the initial substrates by a similar amount to the spread in reactivities as a result of carbon conversion.

The variability in the reactivity toward hydrogenation could be due to either variations in either the reactivity or in the number of $CH_4$ forming sites. The structural order of the carbon substrate may be a major factor with more ordered carbons being less reactive than less ordered ones. It is likely that the structure of the edges of the graphitic sheets determines the reactivity toward hydrogen. An interesting possibility is that carbanionic sites induced by surface salt groups are involved in the hydrogenation mechanism. The alkylation behavior of catalyzed chars has shown that such carbanionic sites exist (*18*). Aromatic carbanions produced by the reaction of alkali metals with aromatic hydrocarbons are known to activate hydrogen (*19*). Hydrogen activation is also observed on alkali metal intercalated graphite and carbons reacted with alkali metal (*20*). These carbanions could activate hydrogen for further reaction with other surface groups or could be the carbon atoms which eventually become hydrogenated to form $CH_4$.

The density of carbanionic sites could vary widely for a given number of surface salts and produce the observed variability in hydrogenation activity. More ordered and converted carbons would be expected to present more ordered surface structures of the type

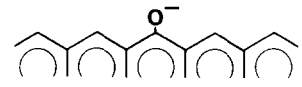


This is especially plausible since potassium catalysts appear to favor retention of the "zigzag" presentation on the edges of graphite layers (*13*). These structures cannot delocalize the charge from the phenoxide to give $\delta^-$ at apical carbons since this charge is directed *ortho-para* (*21*). The surface formed by carbon deposition from the

gas phase might be expected to be more disordered and therefore have a higher density of these carbanionic sites.

ACKNOWLEDGMENTS

We wish to acknowledge helpful conversations with R. Malina at Exxon Research and Engineering, Baytown, Texas, and with Professor John W. Larsen of Lehigh University regarding the role of surface carbanions in methane formation.

REFERENCES

1. For recent reviews see McKee, D. W., *Chem. Phys. Carbon* **16,** 1 (1981); Wood, B., and Sancier, K. M., *Cat. Rev.-Sci. Eng.* **26,** 233 (1984); and relevant papers in the issue of *Fuel* **62**(2), (1983) containing the Proceedings of the International Conference on the Fundamentals of Catalytic Coal Gasification, Amsterdam, Sept. 1982.
2. Holstein, W. L., and Boudart, M., *J. Catal.* **75,** 337 (1982).
3. Lewis, W. K., Gilliland, E. R., and Hipkin, H., *Ind. Eng. Chem.* **45,** 1697 (1953).
4. Cypres, R., Ghodsi, M., and Feron, D., *Thermochim. Acta* **81,** 105 (1984).
5. Gardner, N., Samuels, E., and Wilks, R. H., *Adv. Chem. Ser.* **131,** 217 (1974).
6. Koh, K., *et al.*, U.S. Patent 3,958,957 (1976).
7. Kapteijn, F., and Moulijn, J. A., *J. Chem. Soc.-Chem. Commun.*, 278 (1984).
8. Cabrera, A. L., Heinemann, H., and Somorjai, G. A., *J. Catal.* **75,** 7 (1982).
9. Delannay, F., *et al.*, *Appl. Catal.* **10,** 111 (1984).
10. Mims, C. A., and Pabst, J. K., *J. Phys. Chem.*, to be published.
11. Mims, C. A., and Pabst, J. K., *Amer. Chem. Soc. Div. Fuel Chem, Prepr.* **25,** 258 (1980).
12. Mims, C. A., and Pabst, J. K., *Fuel* **62,** 176 (1983).
13. Mims, C. A., Chludzinski, J. J., Pabst, J. K., and Baker, R. T. K., *J. Catal.* **88,** 97 (1984).
14. Benson, S. W., "The Foundations of Chemical Kinetics," pp. 69–71. McGraw–Hill, New York, 1960; Boudart, M., and Djega-Mariadassou, G., "Kinetics of Heterogeneous Catalytic Reactions," Princeton Univ. Press, Princeton, NJ (1984), pp. 78 ff.
15. Dent, F. J., *J. Chem. Soc. (London)*, (1929), p. 1903.
16. Kapteijn, F., and Moulijn, J. A., *Fuel* **62,** 221 (1983); Freund, H., *Amer. Chem. Soc. Div. Fuel Chem., Prepr.* **30,** 311 (1985).
17. Breisacher, P., and Marx, P. C., *J. Amer. Chem. Soc.* **85,** 3518 (1963).
18. Mims, C. A., Rose, K. D., Melchior, M. T., and Pabst, J. K., *J. Amer. Chem. Soc.* **104,** 6886 (1982).
19. Inokuchi, H., *et al.*, *J. Chem. Phys.* **46,** 837 (1967); Ichikawa, M., and Tamaru, K., *J. Chem. Soc. Faraday Trans. 1* **69,** 1759 (1973).
20. Ishizuka, M., Aika, K.-I., and Ozaki, A., *J. Catal.* **38,** 189 (1975); Boersma, M. A. M., *Cat. Rev.-Sci. Eng.* **10,** 243 (1980).
21. Kornblum, N., Berrinjan, P. J., leNoble, W. J., *J. Amer. Chem. Soc.* **85,** 1141 (1963).